Pergamon

Int. J. Heat Mass Transfer. Vol. 37, No. 17, pp. 2745–2750, 1994

0017-9310/94 $7.00+0.00

0017-9310(94)E0091-8

Efficient calculations of gas radiation from turbulent flames

ROBERT J. HALL† and ALEXANDER VRANOS‡

† UTRC, 411 Silver Lane, East Hartford, CT 06108-1888, U.S.A.
‡ AB Research Associates, South Windsor, CT, U.S.A.

(*Received* 27 *August* 1993 *and in final form* 22 *February* 1994)

Abstract—A calculationally efficient method of calculating time-averaged thermal radiation from flames is presented. The algorithm is derived by ensemble averaging the solution to the equation of radiative transfer. It is shown that, to a good approximation, the local power density can be decorrelated from factors that are functions of path averages. The ensemble averages of path-dependent functions can be calculated using time-averaged properties; the ensemble averages of the local power densities can be carried out by fast numerical quadratures using the local fluctuation probability density function. The result is a predictive technique that requires only one path integration per molecular band. The time-consuming approach of setting up statistical realizations of optical paths, calculating intensity for each realization, and building up the intensity fluctuation statistics is avoided. Sample calculations are given for a turbulent CH_4–H_2 diffusion flame.

1. INTRODUCTION

TURBULENT fluctuations are known to enhance time-averaged radiation from flames relative to predictions based on time-averaged flame properties, and the error arising from neglect of turbulence-radiative interactions can be very large indeed [1–3]. Analytic treatment of turbulence effects on radiation was provided by Kabashnikov and Kmit [1] for the Wien spectral regime and an assumed linear variation of absorption coefficient with gas temperature. Subsequent analysis of the effect in combustion has been mainly numerical in nature. The Monte Carlo modelling approach of refs. [2, 3] divides optical paths into a number of homogeneous, statistically independent elements with dimensions corresponding to the turbulence integral scale, and sets up possible instantaneous realizations of an optical path (Fig. 1). This is usually done in combustion modelling by randomly sampling the mixture fraction distribution function within each homogeneous element, with the underlying probability density function (pdf) parameters derived from a turbulent flow model solution. Assumed state relationships between sampled mixture fraction and temperature/radiating species concentrations, usually taken from laminar flamelet solutions, complete the scheme. The inhomogeneous path parameters are supplied as input to standard radiation band models, and the radiative intensity pdf is built up by performing many trials. This approach of setting up realizations suffers from the time-consuming need to take many trials for good statistics, and may not be practical in modelling complex combustor geometries with large numbers of grid points. A simpler and faster semi-analytic approach for gas radiation is described here, and is found to give good agreement with the more cumbersome Monte Carlo approach. This scheme rests on the demonstration that the local radiant power density can be decorrelated with good accuracy from that part of the local path derivative of absorptivity which depends on path-averaged properties in the Curtis–Godson approximation. Furthermore, the ensemble average of the latter does not differ significantly from a valuc calculated from time-mean properties, since path-averaged properties tend to have reduced fluctuations. A simpler calculation results in which absorptivity derivatives are based on

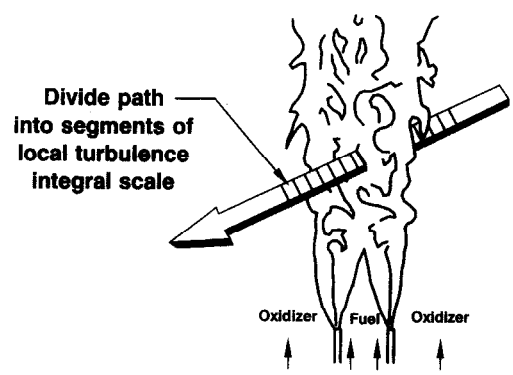

FIG. 1. Representation of a turbulent diffusion flame showing the division of an optical path for radiation into statistically independent segments.

NOMENCLATURE

a	beta density parameter
A	band absorptance
A'	band absorptance derivative
b	beta density parameter
c	constant in stochastic analysis
E_1	exponential integral
f_1, f_2	path-integral functions in stochastic analysis
F	probability density for mixture fraction
H	height above burner surface
I	radiative intensity
I_b	Planck function
m	fuel mixture fraction
m'	fluctuation in mixture fraction
$P(\ )$	normal or Gaussian distribution
P_g	gas pressure
r	correlation coefficient
R_g	gas constant
R_0	fuel tube radius
s	optical pathlength
S/d	line intensity to spacing ratio
T	gas temperature.

Greek symbols

α	integrated band intensity
α_0	integrated band intensity at reference temperature
β	fine structure parameter
γ	parameter in beta density
γ_E	Euler–Mascheroni constant
Γ	gamma function
η_i	probability density parameter
$\Delta\omega$	bandwidth
$\Delta\omega^{(0)}$	bandwidth at $T = 100$ K
ξ	band-intensity path integral
ρ	radiating gas density
σ_1, σ_2	standard deviations of path-integral functions f_1, f_2
τ	transmissivity
ω	frequency
$\omega^{(0)}$	band center frequency.

Subscript

i	ith molecular resonance.

time-averaged properties, and the local radiant power density is ensemble averaged over the mixture fraction pdf using an efficient numerical quadrature. Only one path integration, yielding the time-averaged intensity, is needed for each molecular band. The result is essentially equivalent to Monte Carlo with a great reduction in computation time. The need to perform pdf averaging of the local radiant power density at each node point is no more effort than is ordinarily expended in turbulent flow calculations where ensemble-averaged properties are desired; only one extra such average must be calculated. Numerical examples are presented for a CH_4–H_2 turbulent diffusion flame over a range of optical thicknesses.

2. ANALYSIS

Band models for thermal radiation from combustion products (CO_2, H_2O, CO, ...) are most generally defined in terms of the line intensity to spacing ratio (S/d), and fine structure parameter β, in the Goody model for the wavelength-dependent transmissivity, τ,

$$\tau = \exp\left(\frac{-(S/d)\rho s}{[1+(S/d)\rho s/\beta]^{1/2}}\right) \tag{1}$$

where ρ is the active species density, and s the pathlength. The exponential wideband model [4] specifies (S/d) and β, which for a narrowband model can have a complex frequency dependence, in a particularly simple form. Only four parameters, an integrated band intensity α, band center frequency, $\omega^{(0)}$, the bandwidth $\Delta\omega$, and fine structure parameter independent of frequency are required, namely

$$S/d = \left(\frac{\alpha}{\Delta\omega}\right)\exp\left(-|\omega-\omega^{(0)}|/\Delta\omega\right)$$

$$\beta \neq \beta(\omega). \tag{2}$$

In combustion problems it is usually good approximation to consider the high pressure broadening or large β limit [5] for which the band absorptance A has the form (for homogeneous systems)

$$\frac{A}{\Delta\omega} = \left(\ln\left(\xi/\Delta\omega\right) + E_1\left(\xi/\Delta\omega\right) + \gamma_E\right) \tag{3}$$

where

$$A = \int_0^\infty d\omega\,(1-\tau) \quad \text{and} \quad \xi = \alpha\rho s.$$

Here E_1 is the first exponential integral and γ_E the Euler–Mascheroni constant. Despite its simplicity, the wideband model provides spectrally-integrated intensity predictions sensibly equivalent to those based on more elaborate, narrowband models, and will be adopted here in the analysis to follow. With the usual simplification that the absorption features vary much more rapidly in the vicinity of $\omega^{(0)}$ than the Planck

function, the intensity generated along a line of sight can be represented as

$$I = \sum_i \int_0^s \frac{\mathrm{d}A_i}{\mathrm{d}s'} I_b(s', \omega_i^{(0)})\,\mathrm{d}s' \tag{4}$$

where I_b is the Planck function evaluated at $\omega_i^{(0)}$, and the subscript i denotes the ith active molecular band. Neglecting band overlap effects, the subscript can be suppressed with the understanding that a sum over all bands will be performed at the end.

For nonhomogeneous optical paths, the Curtis–Godson scaling approximation as given by Edwards and Morizumi [5] is employed. In this approximation, the band absorptance is expressed in terms of scaled parameters as

$$\frac{A}{\overline{\Delta\omega}} = \ln(\xi/\Delta\bar{\omega}) + E_1(\xi/\Delta\bar{\omega}) + \gamma_E \tag{5}$$

where

$$\xi = \int_0^s \alpha\rho\,\mathrm{d}s' \tag{6}$$

$$\overline{\Delta\omega} = \frac{1}{\xi}\int_0^s \omega\rho\alpha\,\mathrm{d}s'. \tag{7}$$

Thus, the absorptance derivative is

$$\frac{\mathrm{d}A}{\mathrm{d}\xi} = \frac{\overline{\Delta\omega}}{\xi}(1-\mathrm{e}^{-\xi/\Delta\bar{\omega}}) + \frac{\mathrm{d}\overline{\Delta\omega}}{\mathrm{d}\xi}(E_1(\xi/\Delta\bar{\omega}) + \ln(\xi/\Delta\bar{\omega}) + \gamma_E - 1 + \mathrm{e}^{-\xi/\Delta\bar{\omega}}) \tag{8}$$

where [5]

$$\frac{\mathrm{d}\overline{\Delta\omega}}{\mathrm{d}\xi} = \frac{\Delta\omega - \overline{\Delta\omega}}{\xi}. \tag{9}$$

Our calculations for typical flame conditions indicate that, in practically all situations of interest, it is the first term in equation (8) that dominates, and the second term proportional to the derivative of $\overline{\Delta\omega}$ will be neglected. Thus, we have, finally,

$$I \simeq \int_0^s \left(\frac{\overline{\Delta\omega}}{\xi}\right)(1-\mathrm{e}^{-\xi/\overline{\Delta\omega}})\,\rho\alpha I_b\,\mathrm{d}s'. \tag{10}$$

The quantity of interest is the ensemble average of equation (10). In the integrand, the factor $\rho\alpha I_b$ is point specific, but multiplies an A-derivative factor that involves only path-averaged properties, as per equations (6)–(8). Inasmuch as these paths traverse eddies or volume elements that are presumed to be statistically independent, one can make the approximation that the two factors in the integrand are statistically independent, i.e.

$$\langle I\rangle = \int_0^s \left\langle \frac{\overline{\Delta\omega}}{\xi}(1-\mathrm{e}^{-\xi/\overline{\Delta\omega}})\right\rangle \langle \rho\alpha I_b\rangle\,\mathrm{d}s' \tag{11}$$

where $\langle\ \rangle$ denotes ensemble- or time-averaging.

It will be assumed that state relationships giving temperature T and species densities in terms of the fuel mixture fraction pertain. Central to the modeling process is the concept of a conserved scalar which allows that all fluid properties are, instantaneously, a function of a suitably normalized element mass fraction. This dependence is derived from the laminar diffusion flame model and obviates the need to solve turbulent balance equations for individual species. The set of turbulent flame equations, containing no individual species equations, but only a source-free balance equation for the conserved scalar, can then be solved since the fluid density is a function of the conserved scalar variable only. Species, temperature, and other distributions can be computed by post-processing the output data [6]. Thus, if the probability density $F(m;\eta_i)$ for mixture fraction m is known, where η_i are the known parameters of the pdf, the ensemble average

$$\langle \rho\alpha I_b\rangle = \int_0^1 F(m;\eta_i)\,\rho(m)\alpha(T(m))I_b(T(m))\,\mathrm{d}m \tag{12}$$

can be regarded as a known quantity at each point along the optical path. The crux of the analysis lies in showing that the ensemble average of the other function of path-averaged properties is adequately represented by evaluation of the function with time-averaged properties, i.e.

$$\left\langle \frac{\overline{\Delta\omega}}{\xi}(1-\mathrm{e}^{-\xi/\Delta\bar{\omega}})\right\rangle \simeq \frac{\langle\overline{\Delta\omega}\rangle}{\langle\xi\rangle}(1-\mathrm{e}^{-\langle\xi\rangle/\langle\Delta\bar{\omega}\rangle}). \tag{13}$$

This is equivalent to saying that the time-averaged density enhancement is due mostly to fluctuations in the local emission power density, with the path-dependent attenuation terms averaging out to some extent and making less of a contribution.

The most important bands in CO_2 and H_2O emission have integrated band intensities that are independent of temperature, so it is possible to set $\alpha(T) = \alpha_0$. If the species concentrations $Y_i = Y$ are assumed to be in mass fraction units, the gas law is invoked, and the temperature dependence of $\Delta\omega$ is assumed to be $\Delta\omega^{(0)}\sqrt{(T/100)}$, the function $\mathrm{d}A/\mathrm{d}\xi$ is more simply expressed as

$$A' = \frac{f_2}{(cf_1^2)}(1-\mathrm{e}^{-cf_1^2/f_2}) \tag{14}$$

where

$$\xi = \frac{\alpha_0 P}{R_0}\int \frac{\tilde{W}Y}{\sqrt{(T)}}\,\mathrm{d}s' = \frac{\alpha_0 P}{R_0} f_1$$

$$\overline{\Delta\omega} = \frac{\Delta\omega^{(0)}}{\sqrt{(100)}}\int \frac{\tilde{W}Y}{\sqrt{(T)}}\,\mathrm{d}s' \Big/ \int \frac{\tilde{W}Y}{T}\,\mathrm{d}s' = \frac{\Delta\omega^{(0)}}{\sqrt{(100)}}\frac{f_1}{f_2}$$

$$c = \frac{\alpha_0 P_g\sqrt{(100)}}{R_g\Delta\omega^{(0)}}. \tag{15}$$

Here P_g is the gas pressure, $\tilde{W}$ is the average molec-

ular weight, and R_g is the gas constant. Thus, the statistical average we are seeking can be expressed as

$$\left\langle \frac{f_2}{cf_1^2}(1-e^{-cf_1^2/f_2}) \right\rangle = \langle A' \rangle. \tag{16}$$

The functions f_1 and f_2 are random variables consisting of line integrals along paths which typically will traverse a reasonable number of eddies in which the fluctuations in temperature/concentrations are statistically independent. The fluctuations in f_1 and f_2 are the sum of fluctuations from a number of statistically independent sources. Thus, by the central limit theorem [7], it follows that the probability density functions for f_1 and f_2 will approach normality, irrespective of the form of the fluctuation pdf existing in each source. It is common in turbulent diffusion flame modeling to assume that the local pdf is a beta density [8]. This has been assumed in the numerical examples to follow. The influence of singularities in the beta density on the validity of the central limit theorem has not been examined. It is assumed that pathological cases will occur infrequently, and thus that the normality assumption will be valid in most cases. For those cases where the number of sources is small, the likelihood is that $A' \simeq 1$, and the question possibly is academic. The key question concerns the joint pdf of the functions f_1 and f_2. Monte Carlo techniques involving random sampling of the mixture fraction pdf along optical paths have been employed to calculate the correlation coefficient

$$r = \frac{\langle (f_1 - \langle f_1 \rangle)(f_2 - \langle f_2 \rangle) \rangle}{\sigma_1 \sigma_2} \tag{17}$$

where σ_1 and σ_2 are the standard deviations. For medium conditions and pathlengths of interest, a value close to unity is typically found, indicating a nearly linear relationship between the two

$$\frac{f_2 - \langle f_2 \rangle}{\sigma_2} \simeq \frac{f_1 - \langle f_1 \rangle}{\sigma_1}. \tag{18}$$

The ensemble average of equation (16) can thus be expressed as a function of either f_1 or f_2. Choosing f_1,

$$\langle A' \rangle = c^{-1} \int \frac{f_2(f_1)}{f_1^2}(1-e^{-cf_1^2/f_2(f_1)})P(f_1)\,df_1 \tag{19}$$

where $P(f_1)$ is a normal distribution and f_2 (f_1) is as per equation (18). Equation (19) cannot be calculated easily in closed form, so resort has been made to Gauss–Legendre quadrature. In all cases of interest, it has been found that the prediction of equation (19) does not differ appreciably from that of equation (13), which consists of simply calculating the absorptivity derivative function with ensemble-averaged parameters. This is illustrated in Fig. 2, which shows a comparison of the predictions from equations (13) and (19) as a function of pathlength. The comparison is made for the 2.7 and 6.3 μm transitions in H_2O for representative flame parameters, which are discussed in Figs. 3 and 4. Physically, what seems to be happening is that, to a considerable extent, the path integration averages out the effects of the fluctuations within the sources lying along the path. If statistical properties were spatially uniform, this would be a straightforward application of the ergodic hypothesis.

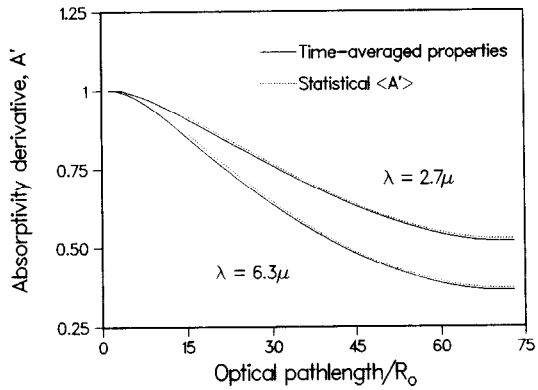

FIG. 2. Comparison of methods of evaluating the absorptivity derivative factor in the equation of radiative transfer solution. The small optical depth asymptote of the statistical evaluation is $A' \to 1$. Flame parameters are as given in Figs. 3 and 4, for $H/R_0 = 200$.

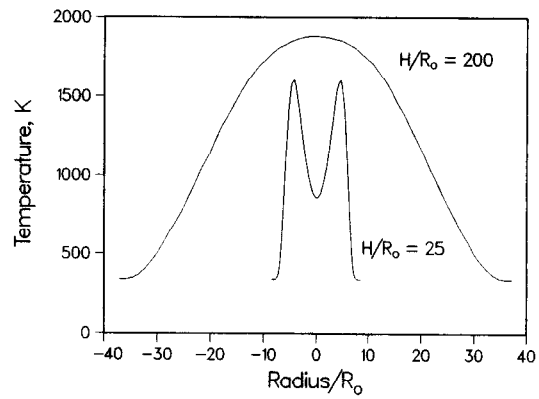

FIG. 3. Time-averaged temperature profiles in a CH_4–H_2/air turbulent diffusion flame as a function of normalized height above the burner.

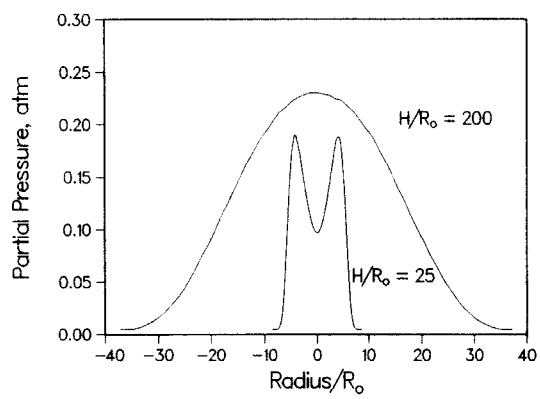

FIG. 4. Time-averaged water vapor partial pressure profiles in a model turbulent diffusion flame.

While this result is intuitively plausible and may not be surprising, it drastically simplifies the job of performing the ensemble average of equation (10). In the optically thin limit, $A' \to 1$, the question is of course moot to begin within.

3. NUMERICAL EXAMPLES

Example calculations have been performed for an atmospheric pressure, CH_4–H_2 turbulent diffusion flame [9]. Radiation measurements have not been performed on this flame, but flow field simulations have been carried out that provide an opportunity to apply the theory developed in this paper to a practical combustion system. The flowfield was simulated with a standard k–ε turbulence model and a parabolic flow solver, providing at each spatial node point the mean fuel mixture and its variance. We assume that the mixture fraction pdf $F(m)$ is described by the beta density [8],

$$F(m) = \frac{\Gamma(a+b)}{\Gamma(a)\Gamma(b)} m^{a-1}(1-m)^{b-1}$$

$$a = \gamma\langle m\rangle$$

$$b = \gamma(1-\langle m\rangle)$$

$$a+b = \gamma$$

$$\gamma = \frac{\langle m\rangle(1-\langle m\rangle)}{\langle m'^2\rangle} - 1 \qquad (20)$$

where Γ is the gamma function, and $\langle m\rangle$ and $\langle m'^2\rangle$ are the mixture fraction mean and variance, respectively. The state relationship between mixture fraction and temperature, density, and species concentrations was assumed to be given by an opposed jet or counterflow flame solution, employing a widely used program [10]. These solutions are characterized by the strain rate, roughly the velocity gradient normal to the flame structure, and a solution corresponding to a median value is used. The k–ε based parabolic code gives a solution in distances normalized by the inner fuel tube radius R_0 (Fig. 1). Line-of-sight radiative flux calculations have been performed at a number of heights from the burner surface. As the flame broadens with increasing height, this has the effect of displaying the effect of increasing optical thickness on the turbulence radiative enhancement, defined as the ratio of the ensemble-averaged intensity to the intensity based on ensemble-averaged properties. The time-averaged temperature and H_2O partial pressure are shown in Figs. 3 and 4 for representative normalized heights above the burner surface. In this flame, the H_2O partial pressure ($\sim$0.25 atm) was so much larger than that of CO_2 ($\sim$0.01 atm) that as a simplifying measure the calculation was confined to H_2O radiation with band-model parameters from [4]. The long-wavelength pure rotational band was neglected. It could be included, but would require a more general formulation of f_1 and f_2 due to the strong temperature dependence of α. The optical paths were divided into segments of length corresponding to the local integral scale. The Monte Carlo calculations were then performed in a way similar to [2, 3]. Within each independent volume element, a random-number generator was used to randomly sample the mixture fraction distribution function [2]. From the resulting value of mixture fraction the instantaneous temperature and species concentrations were then interpolated from the opposed jet state relationships. The intensity for the realization was then calculated from equation (10), summing the active bands. The quantity of interest is the ratio of time-averaged intensity to intensity based on time-averaged properties.

Table 1. Intensity enhancement factors

H/R_0	Monte Carlo	Analytic
25	1.32	1.33
200	1.19	1.20

Table 1 compares the Monte Carlo and 'analytic' predictions for the time-averaged, line-of-sight intensity at two heights above the burner surface. The two heights encompass a significant range of optical thicknesses. As seen, the 'analytic' predictions, which are much more efficiently obtained, satisfactorily agree with the Monte Carlo predictions. There are minor differences in the absolute value of predicted mean properties which have to do with the much different algorithms for the two types of calculations. It should be pointed out that, for the case where the optical path comprises several correlation lengths, the theory of Kabashnikov and Kmit [1] gives an expression equivalent to our equations (11) and (13).

The variation of turbulence enhancement with increasing height above the burner surface is shown in Table 2. The band center optical thickness $\xi/\overline{\Delta\omega}$ of the H_2O 6.3μ transition is shown. As seen, there is not a simple dependence of the fluctuation effect on optical thickness. Intuitively, it could be expected that increasing optical thickness would shield the intensity contributions of more and more eddies, and thus give rise to a reduced fluctuation effect. Low in the flame, the shear and the magnitude of the fluctuations are large, and a relatively large enhancement is seen. As the optical thickness increases, the enhancement effect decreases in accord with the intuitive notion about shielding. However, for very large optical thickness, the enhancement effect starts to increase again because

Table 2. Intensity enhancement factors as a function of optical thickness, $\xi/\overline{\Delta\omega}$

H/R_0	$(\xi/\overline{\Delta\omega})_{6.3\mu}$	Intensity enhancement
25	0.73	1.33
100	1.90	1.14
200	2.54	1.20

the observer sees the effects of only the closest volume elements which are in the high shear region and thus have large fluctuations.

The enhancements of intensity due to radiation are not particularly large in these examples, but this is entirely a function of the particular flame chosen to provide the example. Predicted radiative enhancements will be extremely sensitive to the magnitude of the mixture fraction fluctuations, m'. The purpose of this paper has been to outline a calculational methodology for an effect important in many circumstances.

The fluctuations of individual bands are naturally sensitive to wavelength because the band-center locations on the Planck function generally have different temperature dependences, and thus respond differently to temperature fluctuations. The fluctuations of the 2.7μ band in H_2O, for example, are much larger than those of its 6.3μ band for these flame conditions. Flames in which CO_2 is the dominant radiator can be expected to have different fluctuation properties derived from the temperature sensitivity of the 4.3μ location on the Planck function. The semi-analytic theory also does an accurate job of predicting the standard deviation of the fluctuating fluxes. To the extent that the Monte Carlo technique is successful in predicting the fuel property dependence of the radiation enhancements [2, 3], the procedure given in this paper should be similarly successful, but on a much more efficient basis.

4. CONCLUSIONS

It has been shown by taking ensemble averages of the solution to the equation of radiative transfer that ensemble-averaged thermal radiation intensities from turbulent flames can be calculated in an efficient manner that avoids the time-consuming Monte Carlo approach to the problem. The calculation is essentially recast in terms of properties that can be efficiently averaged over the fluctuation pdf. While the numerical calculations have been for clean flames, there seems little reason to expect that it would not be useful in sooting flames as long as the soot concentrations in adjoining eddies can be regarded as statistically independent. It should be applicable to the individual spectral segments of narrow-band gas radiation models, if their use is preferred.

Acknowledgement—The authors would like to thank Kathi Wicks for her assistance with the preparation of this manuscript.

REFERENCES

1. V. P. Kabashnikov and G. I. Kmit, Influence of turbulent fluctuations on thermal radiation, *J. Appl. Spectrosc.* **31,** 963–967 (1979).
2. J. P. Gore and G. M. Faeth, Structure and spectral radiation properties of turbulent ethylene/air diffusion flames, *Twenty-first Symposium (Int.) on Combustion*, The Combustion Institute, pp. 1521–1531 (1986).
3. M. E. Kounalakis, J. P. Gore and G. M. Faeth, Turbulence/radiation interactions in nonpremixed hydrogen/air flames, *Twenty-second Symposium (Int.) on Combustion*, The Combustion Institute, pp. 1281–1290 (1988).
4. D. K. Edwards and A. Balakrishnan, Thermal radiation by combustion gases, *Int. J. Heat Mass Transfer* **16,** 25–32 (1973).
5. D. K. Edwards and S. J. Morizumi, Scaling of vibration–rotation band parameters for nonhomogeneous gas radiation, *J. Quant. Spectrosc. Radiat. Transfer* **10,** 175–188 (1970).
6. N. Peters, Laminar diffusion flamelet models in nonpremixed combustion, *Prog. Energy Comb. Sci.* **10,** 319–339 (1984).
7. A. Papoulis, *Probability, Random Variables, and Stochastic Processes*. McGraw-Hill, New York (1985).
8. J. Janicka and W. Kollman, A two-variable formalism for the treatment of chemical reactions in turbulent H_2–air diffusion flames, *Seventeenth Symposium (Int.) on Combustion*, The Combustion Institute, pp. 421–429 (1978).
9. A. Vranos *et al.*, Nitric oxide formation and differential diffusion in a turbulent methane–hydrogen diffusion flame, *Twenty-fourth Symposium (Int.) on Combustion*, The Combustion Institute, pp. 377–384 (1992).
10. M. D. Smooke, I. K. Puri and K. Seshadri, A comparison between numerical calculations and experimental measurements of the structure of a counterflow diffusion flame burning diluted methane in diluted air, *Twenty-first Symposium (Int.) on Combustion*, The Combustion Institute, pp. 1783–1792 (1986).